

# Electrical degradation of binary polyethylene blends

A. Gustafsson, M. T. Conde Braña and U. W. Gedde\*

Department of Polymer Technology, The Royal Institute of Technology,  
S-100 44 Stockholm, Sweden

(Received 19 December 1989; revised 9 March 1990; accepted 22 March 1990)

Films of binary mixtures of a low-molecular-mass linear polyethylene (LPE) fraction ( $\bar{M}_m = 2500$ ) and higher-molecular-mass LPE ( $\bar{M}_m = 76\,000$ ) and ethyl-branched PE ( $\bar{M}_m = 150\,000$ ; 1.8 mol% ethyl branches) were exposed to external partial discharges (PD). For both series of binary blends, the average time to breakdown decreased markedly with increasing content of low-molecular-mass LPE component. The PD experiments also showed that rapid cooling was a more favourable thermal treatment than isothermal crystallization at low degree of supercooling. The low-molecular-mass component is the major cause of the electrical breakdown, and electron microscopy showed that rapid cooling promotes co-crystallization between different molecular-mass species. Blends of the low-molecular-mass LPE and the branched PE with intimately mixed components exhibit a resistance towards PD similar to that of the rapidly cooled binary LPE blends. Transmission electron microscopy on a PD exposed, isothermally crystallized binary LPE blend revealed the formation of 100–500 nm wide cracks occurring in the segregated low-molecular-mass domains in the near-surface layer. It is suggested that the inferiority of the low-molecular-mass component is due to its extreme mechanical brittleness, causing a great many cracks to be formed in the surface layer due to thermally induced mechanical stresses caused by the cold plasma.

(Keywords: polyethylene; binary mixtures; morphology; molecular-mass segregation; co-crystallization; electrical degradation)

## INTRODUCTION

It is known from early work by Fava<sup>1</sup> and Fisher<sup>2</sup> that the dielectric strength of polyethylene (PE) increases with decreasing melt index, i.e. increasing molecular mass, and hence it may be postulated that the low-molecular-mass species constitutes the weakest structural unit in this and in other similar semicrystalline polymers. In fact, a number of different authors have presented data in favour of this view<sup>3–7</sup>. Most of these reports deal with the dielectric strength of different microstructural regions with reference to the spherulites. Crystallization of semicrystalline polymers like PE or isotactic polypropylene (PP) is accompanied by molecular-mass segregation<sup>8,9</sup>: the low-molecular-mass species crystallize at a late stage between so-called *dominant* crystal lamellae frequently in the peripheral parts of the spherulites/axialites<sup>10,11</sup>. Model calculations have shown that the tie-chain concentration is significantly lower in the low-molecular-mass segregated domains than elsewhere and this hence constitutes a weak link in the structure<sup>12</sup>.

Wagner<sup>3,4</sup> showed that the discharge channels in thin films of PP subjected to an a.c. field were confined to the spherulite boundaries. This finding was further substantiated by work of Kolesov *et al.*<sup>5,6</sup> showing that the dielectric strength of the material in the centre of a PP spherulite is about double that in the peripheral parts of the spherulites. More recent work by single-needle experiments on PP by Ieda *et al.*<sup>7</sup> shows, on the other hand, that the tree inception voltage increases with increasing spherulite radius and that the tree channels are primarily oriented along the radius of the spherulites,

frequently with a change in direction in the centre of the spherulites.

This paper presents data on the PD resistance of a number of binary mixtures based on a low-molecular-mass linear polyethylene (LPE) sharp fraction and higher-molecular-mass linear and branched PE samples. The morphology of these samples has been studied in detail, and by variation of composition and thermal treatment the low-molecular-mass pseudo-monomodisperse fraction may be either completely segregated or intimately mixed (co-crystallized) with the higher-molecular-mass species.

## EXPERIMENTAL

Single-component samples and binary mixtures based on a linear PE sharp fraction of  $\bar{M}_m = 2500$ ;  $\bar{M}_m/\bar{M}_n = 1.15$  (L2.5) received from Polymer Laboratories Ltd, UK, and two higher-molecular-mass PE samples, both prepared by Neste Polyethylene AB, Sweden, have been studied. Data for the latter polymers were obtained by s.e.c. (RAPRA Technology Ltd, UK) and <sup>13</sup>C n.m.r.: (a) sample L76 is linear and has  $\bar{M}_m = 76\,000$ ,  $\bar{M}_m/\bar{M}_n = 6$ ; (b) sample BE1.8 contains 1.8 mol% of ethyl branches and has  $\bar{M}_m = 150\,000$ ,  $\bar{M}_m/\bar{M}_n = 7$ .

Each binary mixture was made by stirring a hot (120°C) *p*-xylene solution (1.5% (w/w) of polymer) containing both components for at least 20 min, and then rapidly precipitating the polymer in an excess of cold methanol, followed by filtration and drying in vacuum to constant mass. S.e.c. analysis showed that the molecular-mass distributions of the components in the blends were the same as they were prior to blending.

\* To whom correspondence should be addressed

Earlier electron microscopy work<sup>13,14</sup> has demonstrated the adequacy of this mixing technique and any phase separation occurs only on a microscale due to possible molecular fractionation. Single-component samples were treated in the same manner as the binary blends.

Thin films ( $210 \pm 10 \mu\text{m}$ ) were prepared from the different samples by compression moulding at  $150^\circ\text{C}$ . Two main crystallization procedures were used: (a) rapid cooling at  $400^\circ\text{C min}^{-1}$  from  $150$  to  $20^\circ\text{C}$  (referred to as *rapid cooling*); (b) L2.5/L76 samples were cooled from  $150$  to  $123^\circ\text{C}$ , kept at that temperature for 1 h and then rapidly cooled to room temperature (referred to as *isothermally crystallized*). After this preparation all samples were analysed by d.s.c. (Perkin-Elmer DSC-7; melting was recorded at  $10^\circ\text{C min}^{-1}$ ), by polarized light microscopy (Leitz Ortholux Pol BK) on  $10 \mu\text{m}$  thick films given the same thermal treatment as the  $210 \mu\text{m}$  films used for the other analyses and by transmission electron microscopy after chlorosulphonation and staining with uranyl acetate according to the Kanig method<sup>13,14</sup>. Before the electrical testing, the films were coated with a conductive graphite layer on the underside of the sample.

Mass crystallinity ( $w_c$ ) data were obtained by d.s.c. according to the total enthalpy method<sup>15</sup> from:

$$w_c = \Delta h \left( \Delta h^\circ(T_m^\circ) - \int_{T_1}^{T_m^\circ} (c_{pa} - c_{pc}) dT \right)^{-1} \quad (1)$$

where  $\Delta h$  is the measured heat of fusion,  $\Delta h^\circ(T_m^\circ)$  is the heat of fusion of 100% crystalline polymer at the equilibrium melting point, which is equal to  $293 \text{ kJ kg}^{-1}$  (ref. 16), and  $c_{pa}$  and  $c_{pc}$  are the specific heats for the amorphous and crystalline components respectively. Specific heat data of Wunderlich and Baur<sup>17</sup> were used.

The electrical testing involved exposure of the  $210 \pm 10 \mu\text{m}$  films to external partial discharges (PD) by applying an a.c. voltage of  $3.0 \text{ kV}$  at  $1000 \text{ Hz}$  in air at  $23^\circ\text{C}$ . The tests were performed in a specially designed vacuum oven (STW 65, Visimar Ass). The a.c. voltage was controlled by a  $4 \text{ MHz}$  function generator (Model 182A, Wavetek) and a M900 MOSFET power amplifier from HH Electronics. The air gap between the needle electrode (Ogura) and the film was  $1 \text{ mm}$  and the radius of the needle was  $15 \pm 2.5 \mu\text{m}$ . The time to breakdown was recorded by an attached clock. The two-parameter Weibull distribution function,  $1 - F(t) = \exp[-(t/t_{0.63})^b]$ , was fitted to the breakdown time data consisting of at least 15 data points for each sample and the time corresponding to the cumulative frequency  $F = 0.63$  (scale parameter,  $t_{0.63}$ ) and the shape parameter ( $b$ ) were determined by the maximum-likelihood method.

A few sections were taken prior to the final breakdown from samples in the region just beneath the needle electrode and were treated according to the Kanig method<sup>13,14</sup> and studied by TEM.

## RESULTS AND DISCUSSION

Figure 1 presents the melting thermograms of the blends used in this study. The isothermally crystallized blends of L2.5/L76 display bimodal melting, indicating extensive molecular-mass segregation. The high-temperature peak corresponds to the material (L76) that has crystallized at  $123^\circ\text{C}$  and the low-temperature peak is associated with the low-molecular-mass material (L2.5), which has

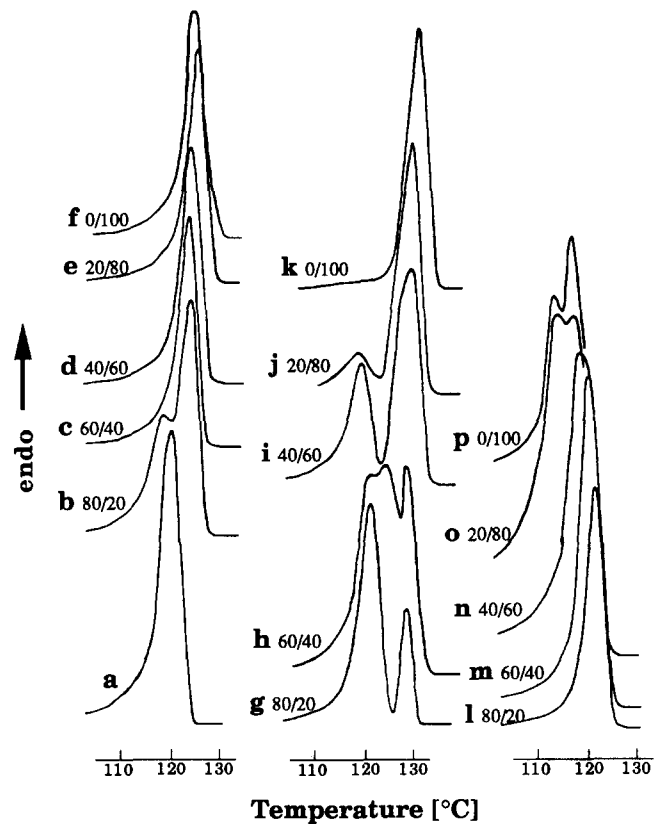
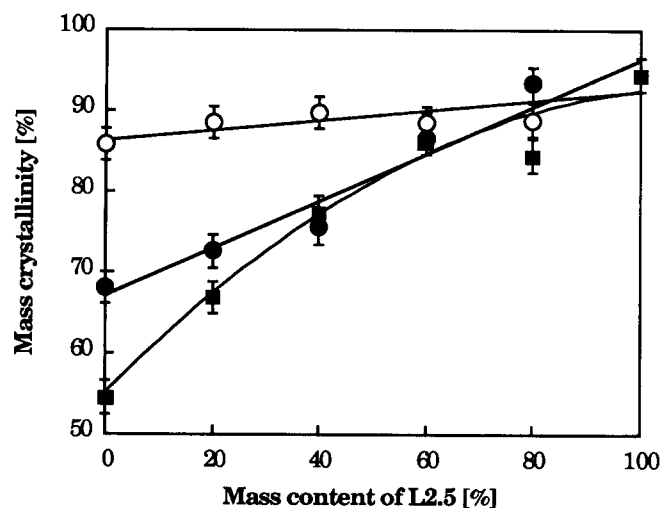


Figure 1 Melting thermograms for the samples studied: (a) L2.5; (b-f) L2.5/L76 rapidly cooled; (g-k) L2.5/LC isothermally crystallized at  $123^\circ\text{C}$ ; (l-p) L2.5/BE1.8 rapidly cooled

crystallized during the cooling phase at lower temperatures. This conclusion is substantiated by the data for the relative sizes of the low-temperature melting peak of these samples: 24.5% (20% L2.5), 42.7% (40% L2.5), 64% (60% L2.5) and 80.6% (80% L2.5). All rapidly cooled L2.5/L76 samples except L2.5/L76 (0.8/0.2) exhibit unimodal melting indicative of a more intimate mixing of the components. L2.5/L76 (0.8/0.2) exhibits two melting peaks at  $121$  and  $127^\circ\text{C}$ , indicating some segregation in this sample. The branched polymer (BE1.8) exhibits a double melting, which is also evident in the L2.5/BE1.8 (0.2/0.8) blend. The other blends based on these polymers display broad but unimodal melting. The d.s.c. data of the L2.5/BE1.8 blends indicate an intimate mixing of the linear and branched PE components.

Figures 2 and 3 present data on mass crystallinity and melting temperatures as a function of composition (percentage of L2.5). The overall trend is that mass crystallinity increases with increasing content of L2.5. The L2.5/L76 blends follow essentially a rectilinear relationship between mass crystallinity and composition. It is evident from these data that the crystallinity of the higher-molecular-mass polymer (L76) makes it more sensitive to the different thermal treatments than L2.5. The L2.5/BE1.8 blends display a non-linear mass crystallinity versus composition relationship (Figure 2). The melting peak temperature of the L2.5/L76 blends decreases with increasing content of L2.5 (Figure 3). The decrease is stronger for the isothermally crystallized samples. This is due primarily to the fact that crystallization becomes progressively slower with increasing low-molecular-mass content, resulting in less crystal thickening and lower final thickness of the L76-rich crystals. The



**Figure 2** Mass crystallinity plotted versus content of L2.5 for the binary blends shown in the figure. ●, L2.5/L76 rapidly cooled; ○, L2.5/L76 isothermally crystallized at 123°C; △, L2.5/L76 isothermally crystallized at 123°C, low-temperature peak; ■, L2.5/BE1.8 rapidly cooled

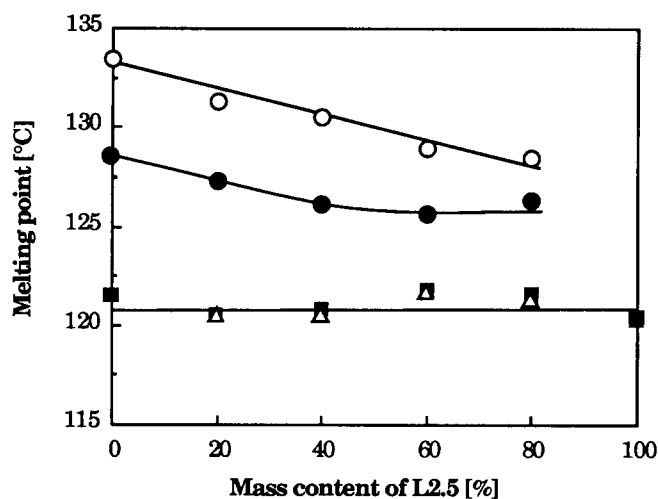


**Figure 3** Melting temperature plotted versus content of L2.5 for: ●, L2.5/L76 rapidly cooled; ○, L2.5/L76 isothermally crystallized at 123°C, high-temperature peak; △, L2.5/L76 isothermally crystallized at 123°C, low-temperature peak; ■, L2.5/BE1.8 rapidly cooled

complete segregation of the L2.5 component in the isothermally crystallized L2.5/L76 blends is further demonstrated by the constant low-temperature melting peak temperature (120°C, i.e. the melting temperature of L2.5) in the whole composition range. The melting peak temperature of the L2.5/BE1.8 blends is  $120 \pm 1^\circ\text{C}$  over the whole range of composition, the same as for the constituents of these blends.

The supermolecular structures of the different blends were revealed by polarized light microscopy and a summary of these data is presented in Table 1. All samples except L2.5 display a spherulitic morphology. The rapidly cooled samples exhibit banded spherulites, the band spacing increasing with increasing content of L2.5. The regularity of the concentric banding decreases with increasing content of L2.5. The isothermally crystallized samples exhibit non-banded spherulites. L2.5 displays as expected an axialitic morphology. All these data are consistent with earlier published data on similar binary PE blends<sup>18</sup>. The spherulite diameter was about the same (25–45  $\mu\text{m}$ ) for the rapidly cooled L2.5/L76 blends irrespective of composition, whereas for the rapidly

cooled L2.5/BE1.8 the spherulite diameter increased continuously with increasing L2.5 content. For the isothermally crystallized L2.5/L76 blend, there is a falling trend in spherulite diameter with increasing content of L2.5.

TEM of chlorosulphonated samples reveals as shown in Figure 4 the lamellar structure. Crystal lamellae appear

**Table 1** Supermolecular structure

Sample	Morphology <sup>c</sup>	$D_s$ ( $\mu\text{m}$ ) <sup>d</sup>	$L_s$ ( $\mu\text{m}$ ) <sup>e</sup>
L76 <sup>a</sup>	BS	30–35	<0.5
L2.5/L76 (0.2/0.8) <sup>a</sup>	BS	30–35	<0.8
L2.5/L76 (0.4/0.6) <sup>a</sup>	BS	25–30	1.0–1.5
L2.5/L76 (0.6/0.4) <sup>a</sup>	BS	25	2.5
L2.5/L76 (0.8/0.2) <sup>a</sup>	IBS	40–45	5
L76 <sup>b</sup>	NBS	50–80	–
L2.5/L76 (0.2/0.8) <sup>b</sup>	NBS	60–80	–
L2.5/L76 (0.4/0.6) <sup>b</sup>	NBS	80–90	–
L2.5/L76 (0.6/0.4) <sup>b</sup>	NBS	30	–
L2.5/L76 (0.8/0.2) <sup>b</sup>	NBS	20	–
BE1.8	BS	5–7	<0.5
L2.5/BE1.8 (0.2/0.8)	BS	15	<0.5
L2.5/BE1.8 (0.4/0.6)	BS	25	1.5
L2.5/BE1.8 (0.6/0.4)	BS	40	1.5
L2.5/BE1.8 (0.8/0.2)	BS	40	3
L2.5	A	80–160	–

<sup>a</sup>Rapidly cooled samples

<sup>b</sup>Isothermally crystallized (123°C) samples

<sup>c</sup>BS = banded spherulites; IBS = irregularly banded spherulites;

NBS = non-banded spherulites; A = axialites

<sup>d</sup>Spherulite diameter or axialite length

<sup>e</sup>Band spacing

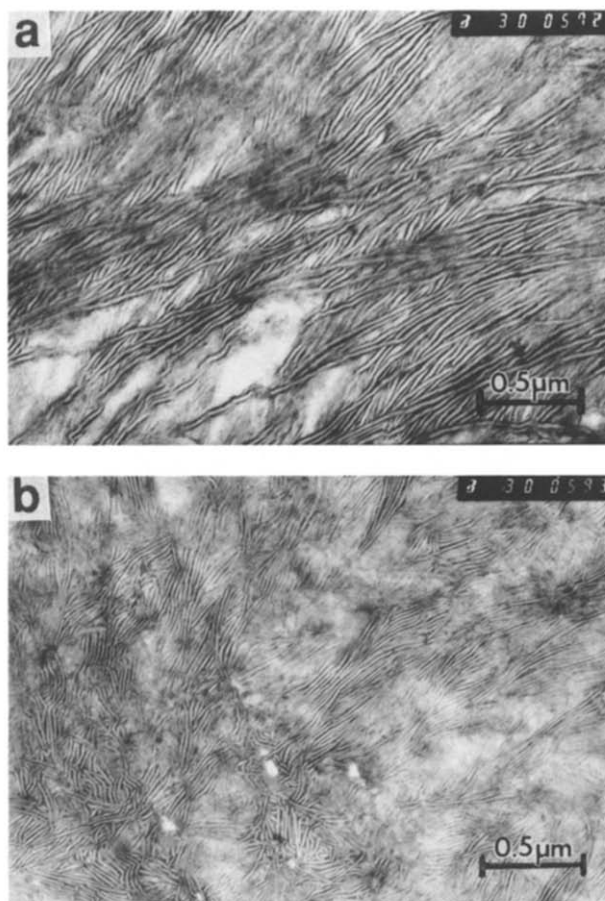


**Figure 4** Transmission electron micrographs of chlorosulphonated samples: (a) L2.5/L76 (0.4/0.6), isothermally crystallized at 123°C; (b) L2.5/L76 (0.4/0.6), rapidly cooled from the melt

light and amorphous interlayers appear dark. A very 'helpful' property of the L2.5 component is that it cannot be stained using the Kanig method<sup>19</sup>. No contrast between the amorphous and crystalline phases is obtained. This has also been reported earlier by Stack *et al.*<sup>20</sup> on similar samples. Thus, the presence of isolated domains of L2.5 material in the blends is easily distinguished as white spots. There is, however, another cause for the absence of contrast. If the stained surfaces of the crystal lamellae are tilted with respect to the beam, their contours gradually disappear and the contrast is lost. However, it was established by tilting the specimens that this was not the case for the L2.5/L76 (0.4/0.6) crystallized at 123°C. The dominant feature of this sample, shown in *Figure 4a*, is the occurrence of relatively long and well defined dominant lamellae surrounding areas apparently without lamellae. These dominant lamellae are most probably composed of material rich in L76, whereas the zones lacking lamellar structure are obviously composed of material rich in L2.5, forming non-stainable subsidiary lamellae. A feature of this sample is the holes inside the white zones probably created by the sectioning process. This is due to the brittleness of L2.5, the low-molecular-mass material.

The rapidly cooled L2.5/L76 blends were also studied by TEM (*Figure 4b*). The temperature at which these samples (L76 and L76/L2.5 0.4/0.6) crystallize is about  $107 \pm 2^\circ\text{C}$ , which corresponds to a supercooling of 36–38°C. Careful examination of a number of micrographs taken from the rapidly cooled L2.5/L76 (0.4/0.6) blend shows that non-lamellar areas constitute only a small part of the total sample area, of the order of a few per cent. This sample also showed similar holes inside the white spots as the sample of the same composition crystallized at 123°C. It should be pointed out, however, that this feature of holes is not dominant in the rapidly cooled blend and that the concentration of cracks and L2.5-rich material is significantly lower in the rapidly cooled blend than in the corresponding sample crystallized at 123°C.

*Figure 5* presents histograms of L2.5/L76 (0.4/0.6) both isothermally crystallized (IC) and rapidly cooled (RC) from the melt. The histograms are obtained from direct measurement of the crystal and amorphous regions in the TEM micrographs according to a procedure described in ref. 14. A major difference between the two samples was that the average crystal thickness is 70% greater in the IC sample (average crystal thickness  $\langle L_c \rangle = 16.8 \text{ nm}$ ) than in the RC sample ( $\langle L_c \rangle = 10 \text{ nm}$ ), primarily because crystallization was carried out at a higher temperature in the former sample. Both crystal thickness distributions were unimodal as expected based on the melting thermograms, since, in the IC sample, crystals consisting of L2.5 constituting the low-temperature melting peak are not included in the histograms. Another difference between the two samples concerns the amorphous interlayer. The average thickness is lower in the RC sample, 7.9 nm compared with 8.7 nm in the IC sample, a fact which indicates that, in the RC sample, the low-molecular-mass component (L2.5) is to some extent included in the crystals together with the L76 polymer. These average values are each based on approximately 300 single values and the difference between the two is, despite being small, significant.

TEM data for the L2.5/BE1.8 blends are published in another paper<sup>21</sup>. The absence of white unstained spots

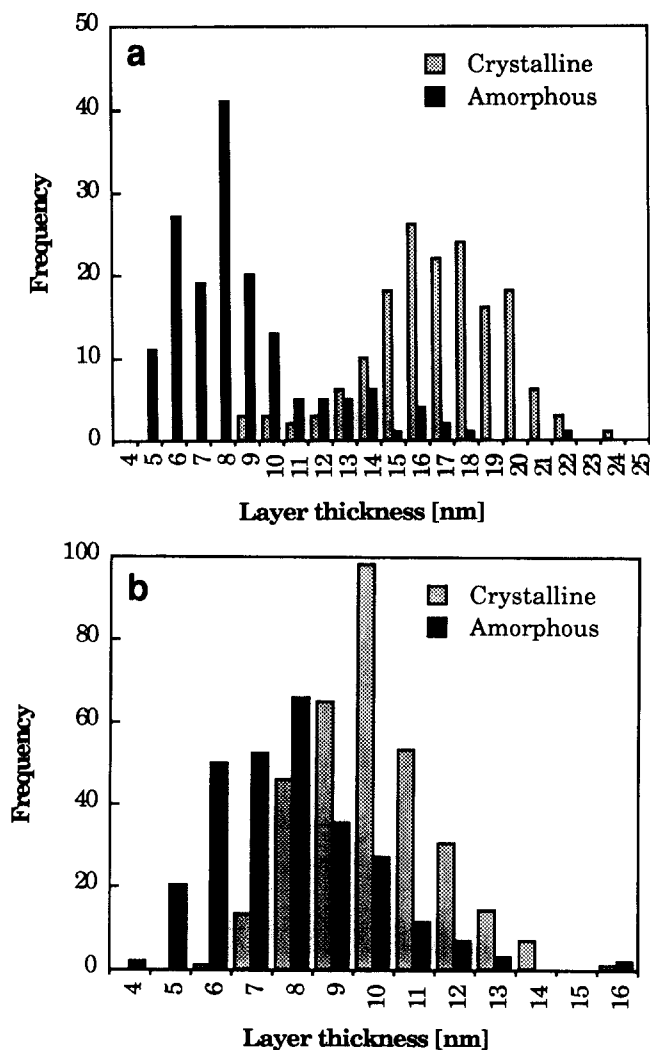


**Figure 5** Histograms showing data for the crystalline and amorphous interlayer thickness: (a) L2.5/L76 (0.4/0.6), isothermally crystallized at 123°C; (b) L2.5/L76 (0.4/0.6), rapidly cooled from the melt

and the uniform lamellar structure (i.e. thickness of amorphous layer and local crystallinity) in these samples constitute the experimental evidence in favour of co-crystallization of the components. The major effect of the introduction of L2.5 is a decrease in the average amorphous thickness from about 15 nm in the pure BE1.8 to about 5 nm in L2.5/BE1.8 (0.8/0.2), which is clearly evidence in support of co-crystallization between L2.5 and BE1.8.

Based on data by d.s.c., TEM and polarized light microscopy, the following conclusions may be drawn with regard to the morphology of the binary mixtures. The isothermally crystallized L2.5/L76 blends display pronounced molecular-mass segregation. Stacks of dominant lamellae of L76 surround subsidiary lamellae of L2.5. The number of dominant lamellae in a stack depends on the composition. It has been shown in a previous paper<sup>22</sup> that the number of dominant lamellae in a stack increases with decreasing content of L2.5. Spherulites are the dominant morphology observed in these samples. Only L2.5 displayed an axialitic morphology. In the rapidly cooled L2.5/L76 samples the components are more intimately mixed. The frequency of domains with low-molecular-mass material is much lower than in the corresponding isothermally crystallized samples. Blends of L2.5/BE1.8 are intimately mixed and

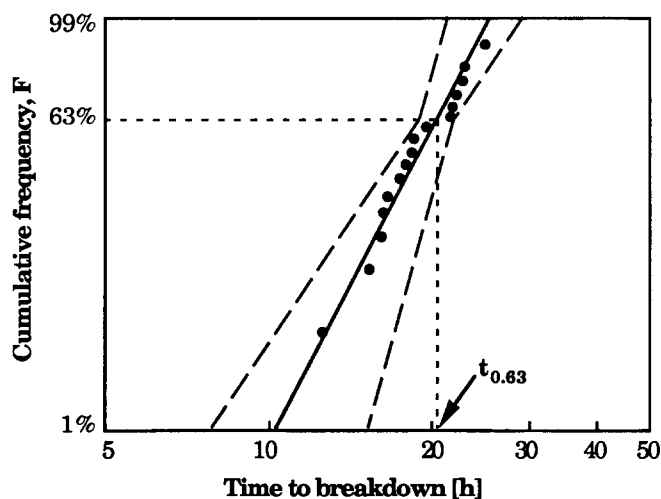


**Figure 6** Time to breakdown data for rapidly cooled L76 (100%) presented in a Weibull plot with 95% confidence limits showing the scale parameter ( $t_{0.63}$ ) calculated from  $\ln\{\ln[1/(1-F)]\} = b(\ln t - \ln t_{0.63})$

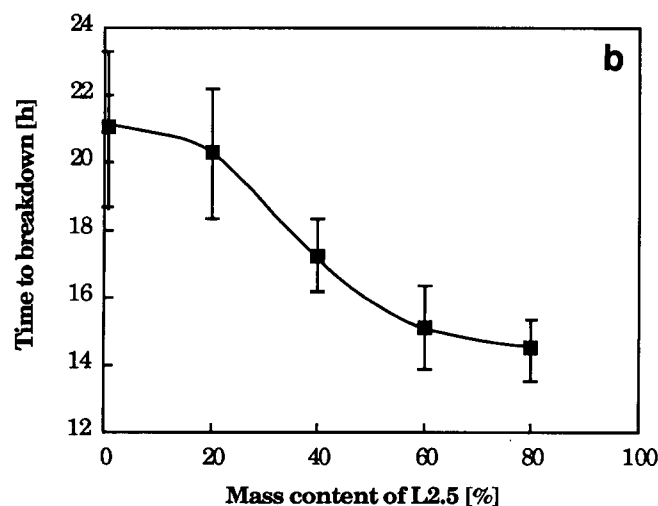
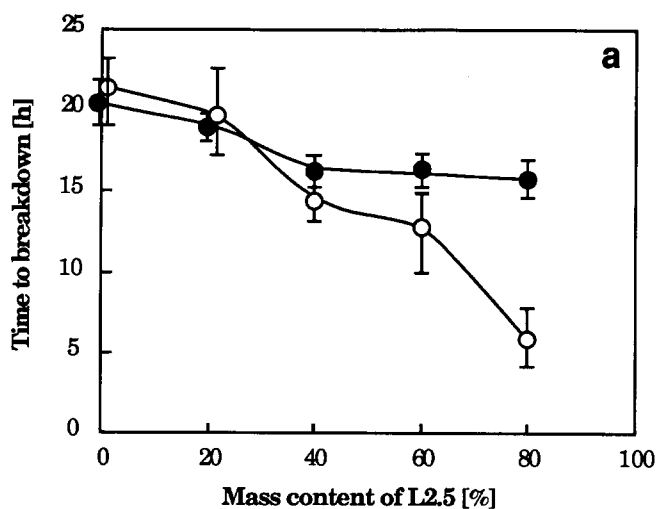


**Figure 7** Time to breakdown ( $t_{0.63}$ ) plotted as a function of content of L2.5 in binary blends: (a) L2.5/L76, isothermally crystallized at 123°C (○); L2.5/L76, rapidly cooled (●); (b) L2.5/BE1.8, rapidly cooled. The bars refer to the 95% confidence limits

the components crystallize together in the same crystal lamellae. All these blends display banded spherulites.

Data for the PD resistance are presented in *Figures 6* and *7* and *Table 2*. The high value of the shape parameter

(*b*) demonstrates the low scattering in the data. The *b* parameter is generally higher for the rapidly cooled blends than for the isothermally crystallized blends. Furthermore, the *b* parameter decreases with increasing content of L2.5 in the isothermally crystallized L2.5/L76 blends (*Table 2*). The general trend is that samples displaying a low *b* value also exhibit a low average life ( $t_{0.63}$ ) (*Table 2* and *Figure 7*). For all blends a decrease in average life ( $t_{0.63}$ ) is observed with increasing content of the low-molecular-mass component (*Figure 7*). The isothermally crystallized samples of L2.5/L76 containing segregated low-molecular-mass species exhibit the lowest PD resistance of all samples. The rapidly cooled samples of L2.5/L76 and L2.5/BE1.8 exhibit the same PD resistance. The average lifetime for the pure L2.5 component was found to be about 2 h, i.e. one order of magnitude shorter than the corresponding lifetime of the pure high-molecular-mass samples (L76 and BE1.8).

*Figures 8* and *9* present data by TEM for samples subjected to PD just prior to breakdown. A surface layer, 1–10  $\mu\text{m}$  thick, containing a great many 100–500 nm long cracks has developed in the L2.5/L76 (0.4/0.6) blend (*Figure 8*). The openings (cracks) appear as completely white spots on the micrographs. These areas are clearly different from the white spots that are due to the segregated, low-molecular-mass material. Apart from the frequent void opening occurring in the segregated low-molecular-mass regions, the effect on the lamellar structure seems to be limited. The crystalline and amorphous layer thicknesses have not been affected by the PD exposure (cf. *Figures 5* and *9*). The following average values were obtained:  $\langle L_c \rangle = 16.8$  nm,  $\langle L_a \rangle = 8.7$  nm (prior to PD exposure);  $\langle L_c \rangle = 16.4$  nm,  $\langle L_a \rangle = 8.8$  nm (after PD exposure). The cracks may have been formed either as a direct consequence of the PD treatment or due to embrittlement of the polymer due to the PD plasma and fracture at a later stage during sectioning of the sample. A mixture of these two causes is the most probable explanation.

## CONCLUSIONS

Films of binary mixtures of a low-molecular-mass linear PE fraction ( $\bar{M}_m = 2500$ ) and higher-molecular-mass linear ( $\bar{M}_m = 76000$ ) and ethyl branched PE ( $\bar{M}_m =$

**Table 2** Data for the shape parameter (*b*) of the two-parameter Weibull distribution function

Sample	<i>b</i> parameter
L76 (RC) <sup>a</sup>	6.7
L2.5/L76 (0.2/0.8) (RC)	10.3
L2.5/L76 (0.4/0.6) (RC)	9.8
L2.5/L76 (0.6/0.4) (RC)	8.9
L2.5/L76 (0.8/0.2) (RC)	7.4
L76 (IC) <sup>b</sup>	6.5
L2.5/L76 (0.2/0.8) (IC)	4.6
L2.5/L76 (0.4/0.6) (IC)	7.4
L2.5/L76 (0.6/0.4) (IC)	4.1
L2.5/L76 (0.8/0.2) (IC)	2.3
BE1.8 (RC)	4.6
L2.5/BE1.8 (0.2/0.8) (RC)	5.5
L2.5/BE1.8 (0.4/0.6) (RC)	7.9
L2.5/BE1.8 (0.6/0.4) (RC)	6.3
L2.5/BE1.8 (0.8/0.2) (RC)	9.2

<sup>a</sup>Rapidly cooled

<sup>b</sup>Isothermally crystallized at 123°C

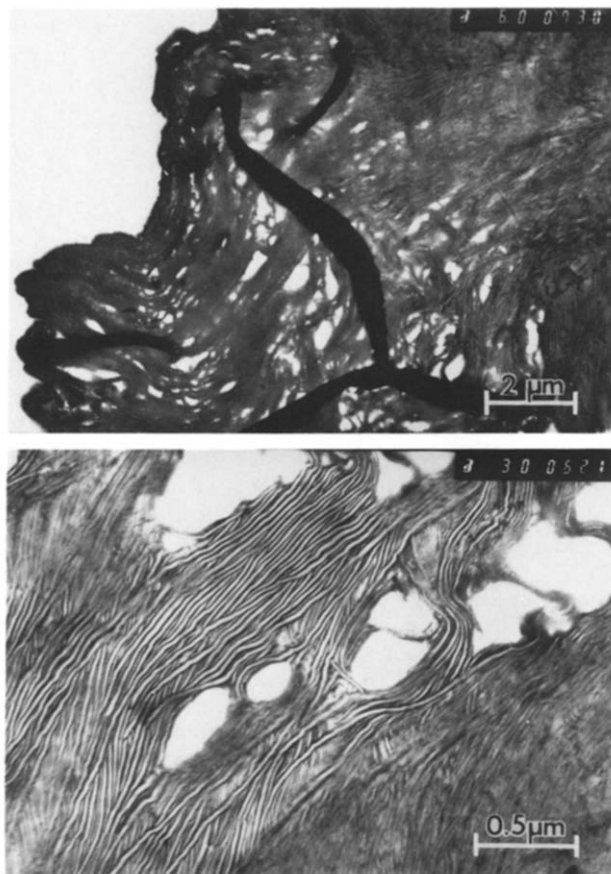


**Figure 8** Transmission electron micrographs of chlorosulphonated sample taken from the near-surface layer of a PD exposed film of isothermally crystallized (123°C) L2.5/L76 (0.4/0.6). The lower micrograph is a magnification from the porous surface layer

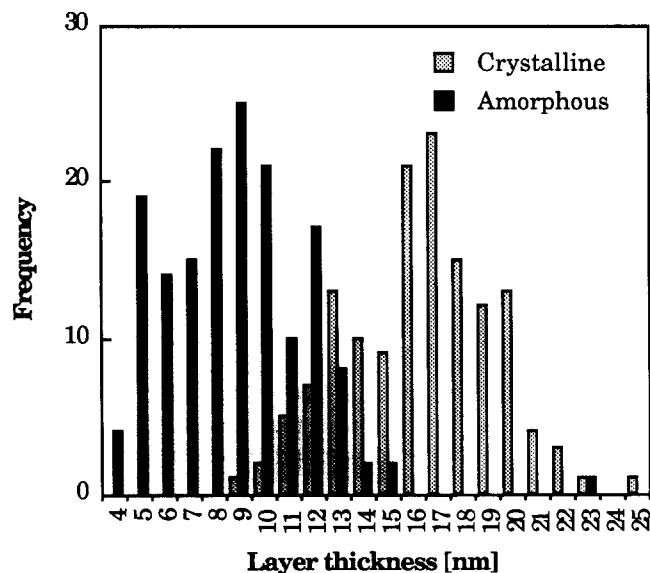


**Figure 9** Histogram showing data for the crystalline and amorphous interlayer thickness for the surface layer of a PD exposed sample of isothermally crystallized (123°C) L2.5/L76 (0.4/0.6)

150 000, 1.8 mol% ethyl branches) have been exposed to external partial discharges (PD). For both series of binary blends, the average time to breakdown decreased markedly with increasing content of low-molecular-mass LPE component. The PD experiments also showed that rapid cooling was a more favourable thermal treatment than isothermal crystallization at low degree of supercooling. The PD resistance of the low-molecular-mass component

(L2.5) is thus significantly lower than that of the higher-molecular-mass linear and branched components. The presence of isolated domains of the low-molecular-mass component decreases the PD resistance more than if the latter is intimately mixed (co-crystallized) with the higher-molecular-mass component. The inferiority of the low-molecular-mass component may be due to its low mechanical strength. Isolated domains of the low-molecular-mass component exhibit extreme brittleness due to their complete absence of interlamellar tie chains. Partial discharges produce a cold plasma, which consists of electrons, ions and other reactive species causing radical processes to occur in the amorphous phase of the polymer. The high crystallinity of the linear low-molecular-mass component may seem advantageous in this respect. However, dissipation processes in the surface layer cause thermally induced mechanical stresses, which, if the material is brittle, may induce cracking and a shortened life of the polymer. The TEM findings in the PD exposed sample, which reveals the formation of 100–500 nm cracks in the low-molecular-mass domains in the surface layer, substantiate this hypothesis.

#### ACKNOWLEDGEMENTS

This study has been sponsored by the National Swedish Board for Technical Development (STU) via Grant 84-03454P and ABB Corporate Research, Västerås, Sweden. The authors wish to thank Neste Polyethylene AB, Sweden, for supplying the polyethylene grades used in this study and L. Johansson, U. Gäfvert, T. Schütte and A. Hjortsberg at ABB Corporate Research, Västerås, Sweden, for valuable discussions.

#### REFERENCES

- 1 Fava, R. A. *Proc. IEE* 1965, **112**, 819
- 2 Fisher, P. Ann. Rep. CEIDP 1975, National Academy of Sciences – NRC, Washington, DC, p. 661
- 3 Wagner, H. *Elektrotechn. Z. Ausg. (A)* 1973, **94**, 436
- 4 Wagner, H. Ann. Rep. CEIDP 1975, National Academy of Sciences – NRC, Washington, DC, p. 62
- 5 Kolesov, S. N., Balaban, N. P. and Kheraskov, L. N. *Vysokomol Soed. (B)* 1970, **12**, 366
- 6 Kolesov, S. N. and Kheraskov, L. N. *Vysokomol Soed. (B)* 1970, **12**, 266
- 7 Ieda, M., Navata, M. and Kawamura, H. Proc. 4th Int. Symp. on High Voltage Engineering, Athens, Greece, 1983
- 8 Gedde, U. W. and Jansson, J.-F. *Polymer* 1983, **24**, 1521
- 9 Gedde, U. W., Eklund, S. and Jansson, J.-F. *Polymer* 1983, **24**, 1532
- 10 Winram, M. M., Grubb, D. T. and Keller, A. *J. Mater. Sci.* 1978, **13**, 791
- 11 Gedde, U. W. and Jansson, J.-F. *Polymer* 1984, **25**, 1263
- 12 Gedde, U. W. and Jansson, J.-F. *Polymer* 1985, **26**, 1469
- 13 Rego Lopez, J. M., Conde Braña, M. T., Terselius, B. and Gedde, U. W. *Polymer* 1988, **29**, 1045
- 14 Conde Braña, M. T., Iragorri Sainz, J. I., Terselius, B. and Gedde, U. W. *Polymer* 1989, **30**, 411
- 15 Blundell, D. J., Beckett, D. R. and Willcocks, P. H. *Polymer* 1981, **22**, 704
- 16 Wunderlich, B. 'Macromolecular Physics', Vol. 3, Academic Press, New York, 1980
- 17 Wunderlich, B. and Baur, H. *Adv. Polym. Sci.* 1970, **7**, 151
- 18 Rego Lopez, J. M. and Gedde, U. W. *Polymer* 1988, **29**, 1037
- 19 Conde Braña, M. T., Terselius, B. and Gedde, U. W. unpublished data
- 20 Stack, G. M., Mandelkern, L. and Voigt-Martin, I. G. *Macromolecules* 1984, **17**, 321
- 21 Conde Braña, M. T. and Gedde, U. W. *Polymer* submitted for publication
- 22 Conde Braña, M. T., Iragorri Sainz, J. I. and Gedde, U. W. *Polym. Bull.* 1989, **22**, 277